Homogenization of periodic elastic composites and locally resonant sonic materials

Sia Nemat-Nasser
Department of Mechanical and Aerospace Engineering, University of California, San Diego, La Jolla, CA 92037-0415, USA

John R. Willis
Department of Applied Mathematics and Theoretical Physics, Centre for Mathematical Sciences, Wilberforce Road, Cambridge CB3 0WA, United Kingdom

Ankit Srivastava* and Alireza V. Amirkhizi
Department of Mechanical and Aerospace Engineering, University of California, San Diego, La Jolla, CA 92037-0415, USA
(Received 13 July 2010; revised manuscript received 14 December 2010; published 18 March 2011)

A method for homogenization of an elastic composite with periodic microstructure is presented, focusing on the Floquet-type elastic waves. The resulting homogenized frequency-dependent elasticity and mass density then automatically satisfy the overall conservation laws and by necessity produce the exact dispersion relations. It is also shown that the dispersion relations and the associated field quantities can be accurately calculated using a mixed variational approach, based on the microstructure of the associated unit cell. The method is used to calculate the dynamic effective parameters for a layered composite by using both the exact solution and the results of the mixed variational formulation. The exact and approximate results are shown to be in close agreement, which makes it possible to use the approximate method for the proposed type of homogenization in cases where an exact solution does not exist. The homogenized frequency-dependent effective parameters give rise to the concept of dynamic Ashby charts that can be used to illustrate the effect of the microstructural architecture on the dynamic properties of a composite. In particular, the charts vividly display how this effective stiffness and density vary with frequency and may attain negative values within certain frequency ranges which can be changed as desired using the microarchitecture while keeping the volume fraction of the unit cell's constituents constant.

DOI: 10.1103/PhysRevB.83.104103 PACS number(s): 43.20.Gp, 43.20.Jr, 62.20.D−

I. INTRODUCTION

There has been a recent surge of interest in the field of the dynamic response of composites with tailor-made microstructure. By controlling the microstructural heterogeneities in a periodic composite, exotic dynamic responses at the macroscale can be achieved. This necessitates developing systematic homogenization procedures by which the dynamic behavior of periodic composites can be expressed in terms of averaged parameters such as effective compliance and effective density. For wavelengths that are suitably larger than the scale of heterogeneity, these homogenized material parameters are expected to provide an effective description of the dynamic behavior of the composite. At a minimum, one must ensure that the resulting effective parameters satisfy (1) the overall conservation laws and compatibility relations, and (2) the composite's dispersion relations. These dispersion relations can be accurately and independently calculated based on the microstructure of the unit cell, as we discuss in this paper. Our focus in this work is on Floquet-type harmonic waves in periodic elastic composites.

For Floquet- or Bloch-type electromagnetic waves in periodic media, Refs. 1–3 gave a method of homogenization, using surface and line integrals of field variables. The authors pointed out that the effective parameters calculated by their method exhibit spatial dispersion for a homogeneous case and corrected for this by removing the factor introduced by finite differencing (FD) of Maxwell's equations; for this, they use the calculated dispersion relation together with first-order corrected expressions for the effective permittivity and permeability. The FD method was also applied to study chiral media.[4] In Ref. 4, the effective permittivity, permeability, and chirality tensors are independently corrected up to the first order in the normalized wave number (phase advance), and similarly, the associated dispersion relations are corrected. The method we present in the present paper does not require any such correction and in fact the corresponding results as a matter of course satisfy the above-mentioned two requirements exactly. In Ref. 5 the authors have given a microstructurally based homogenization technique for calculating effective electromagnetic properties in which the values of the field variables in the unit cell are not required and their results do satisfy the above-stated two basic requirements. Based on an ensemble averaging technique, Ref. 6 presented a general method in which the displacement was driven by a nonrandom body force, thus allowing one to consider a mean wave with independent wave number and frequency. In this approach, the local field equations for the mean wave are ensured to be satisfied by the presence of the body force. When the body force is zero, then the dispersion relation results, which relates the wave number and frequency. In this manner, Willis calculated the effective elastodynamic parameters for laminated media using Green's function. These effective parameters satisfy the dispersion relation and are spatially nondispersive in the long-wavelength limit. Here we present an analogous approach for calculating effective elastodynamic parameters $(C^{\text{eff}}, \rho^{\text{eff}})$ for Floquet waves in periodic elastic composites. The method presented in this paper involves writing the field equations locally through a single unit cell as a function of position and averaging the equation with respect to the position

variable over the unit cell. The method proposed by Willis[6] involves a random medium and creates an average of statistical ensembles. The two methods result in identical homogenized parameters for Bloch-type waves in periodic composites, satisfying the dispersion relation by necessity. This method is used to calculate the effective parameters for a two-layered composite by using the exact solution[7] and an approximate mixed variational method.[8–10] The efficacy and accuracy of the approximate method were demonstrated by means of numerical examples,[8–10] using Fourier series approximation. The convergence of the method was subsequently proven.[11] It was shown that while the rate of convergence of both the Rayleigh quotient and the mixed formulation depends on the regularity of the elastic properties and the density through the unit cell, the mixed formulation always has a convergence rate faster than that of the Rayleigh quotient. Here we show, by way of a two-layered example, that dispersion results obtained by using the approximate method quickly converge to the exact solution. The displacement and stress fields thus calculated from the approximate method are used to calculate the effective overall parameters, and it is shown that the results converge to the results of the homogenization calculations based on the exact solution. This is done with the view of subsequently using the approximate method to homogenize composites with more complex microstructures where exact expressions for the field quantities and the dispersion relations do not exist.

The effective parameters thus calculated are functions of frequency. An efficient and logical way of representing them is by multidimensional graphs which we call dynamic Ashby charts. These charts are extensions of the standard Ashby charts,[12] in which the frequency (or wave vector) forms an additional axis. We illustrate how these charts may be used to tailor the effective dynamic properties of heterogeneous composites using architectural design of the microstructure. We show that by using the same volume fraction of constituents within a unit cell but varying the cell's microarchitecture, composites of vastly different dynamic properties can be created, e.g., composites that for Floquet-type waves may display negative effective mass density and/or negative effective stiffness, as well as negative index of refraction over a certain desired frequency range.

It was shown in Ref. 13 that hypothetical materials with negative index of refraction, if realized, would possess exotic electromagnetic properties. These materials exhibit group velocity which is antiparallel to phase velocity and which was experimentally realized.[14] "Negative" electromagnetic response of materials is a result of local substructural resonances in electric and magnetic fields. Analogous elastic materials with antiparallel group velocity have been proposed.[15–17] The central idea was to use local resonances from rigid-body motions to create low-frequency bands of negative group velocity. We present a four-layered structural composite which uses this idea and exhibits a low-frequency negative passband. Indeed, elastic composites consisting of very stiff inclusions periodically embedded in a relatively soft matrix do display negative branches, as can be seen from the results presented in the literature.[10]

We mention that periodic lattices with interesting overall dynamic properties that result from wave interaction with local microstructure have been extensively studied; see, e.g., Ref. 18 and references cited therein. In particular, Ref. 19 discusses multiscale microstructural designs to alter and control the material's overall frequency band structure and other related dynamic properties.

In what follows, we first present a general variational method that yields accurate eigenvalues and eigenmodes for periodic composites whose corresponding unit cell consists of constituents with discontinuous properties. Then we use the results to calculate the frequency-dependent effective stiffness and mass density of a two-layered composite, comparing the results with those based on the exact solution of the field equations. Finally, we present the concept of the dynamic Ashby chart and illustrate this for a two-layered composite, demonstrating the effect of microstructural design on the dynamic response of the composite.

II. MIXED METHOD FOR CALCULATION OF EIGENMODES OF PERIODIC COMPOSITES

Consider harmonic waves in an unbounded periodic elastic composite consisting of a collection of unit cells, Ω. In view of periodicity, we have $\rho(\mathbf{x}) = \rho(\mathbf{x} + m' I^\beta)$ and $C_{jkmn}(\mathbf{x}) = C_{jkmn}(\mathbf{x} + m' I^\beta)$, where $\mathbf{x}$ is the position vector with components $x_j, j = 1,2,3$, $\rho(\mathbf{x})$ is the density, and $C_{jkmn}(\mathbf{x})$ $(j,k,m,n = 1,2,3)$ are the components of the elasticity tensor in Cartesian coordinates. m' is any integer and $I^\beta, \beta = 1,2,3$, denote the three vectors which form a parallelepiped enclosing the periodic unit cell.

For time harmonic waves with frequency ω $(\lambda = \omega^2)$, the field quantities are proportional to $e^{\pm i\omega t}$. The field equations become

$$\sigma_{jk,k} + \lambda\rho u_j = 0, \quad \sigma_{jk} = C_{jkmn} u_{m,n}. \tag{1}$$

For harmonic waves with wave vector $\mathbf{q}$, the Bloch boundary conditions take the form

$$u_j(\mathbf{x} + I^\beta) = u_j(\mathbf{x}) e^{i\mathbf{q}\cdot I^\beta}, \quad t_j(\mathbf{x} + I^\beta) = -t_j(\mathbf{x}) e^{i\mathbf{q}\cdot I^\beta} \tag{2}$$

for $\mathbf{x}$ on $\partial\Omega$, where $\mathbf{t}$ is the traction vector.

To find an approximate solution of the field equations [Eq. (1)] subject to the boundary conditions [Eq. (2)], we consider the following expressions:

$$\bar{u}_j = \sum_{\alpha,\beta,\gamma=-M}^{+M} U_j^{(\alpha\beta\gamma)} f^{(\alpha\beta\gamma)}(\mathbf{x}), \tag{3}$$

$$\bar{\sigma}_{jk} = \sum_{\alpha,\beta,\gamma=-M}^{+M} S_{jk}^{(\alpha\beta\gamma)} f^{(\alpha\beta\gamma)}(\mathbf{x}), \tag{4}$$

where the approximating functions $f^{(\alpha\beta\gamma)}$ are continuous and continuously differentiable, satisfying the Bloch periodicity conditions. As shown in Ref. 8, the eigenvalues are obtained by rendering the following functional stationary:

$$\lambda_N = (\langle \sigma_{jk}, u_{j,k} \rangle + \langle u_{j,k}, \sigma_{jk} \rangle - \langle D_{jkmn}\sigma_{jk}, \sigma_{mn} \rangle) / \langle \rho u_j, u_j \rangle, \tag{5}$$

where $\langle g u_j, v_j \rangle = \int_\Omega g u_j v_j^* \, dV$, where the star denotes the complex conjugate, and D_{jkmn} are the components of the elastic compliance tensor, the inverse of the elasticity tensor C_{jkmn}.

Substituting Eqs. (3) and (4) into Eq. (5) and equating to zero the derivatives of λ_N with respect to the unknown coefficients $U_j^{(\alpha\beta\gamma)}$ and $S_{jk}^{(\alpha\beta\gamma)}$, we arrive at the following set of linear homogeneous equations:

$$\langle \bar{\sigma}_{jk,k} + \lambda_N \rho \bar{u}_j, f^{(\alpha\beta\gamma)} \rangle = 0,^1 \quad \langle D_{jkmn}\bar{\sigma}_{mn} - \bar{u}_{j,k}, f^{(\alpha\beta\gamma)} \rangle = 0.^2 \tag{6}$$

There are $6M_p^3$ ($M_p = 2M + 1$) equations in Eq. $(6)^2$ for a general 3-directionally periodic composite. They may be solved for $S_{jk}^{(\alpha\beta\gamma)}$ in terms of $U_j^{(\alpha\beta\gamma)}$ and the result substituted into Eq. $(6)^1$. This leads to a system of $3M_p^3$ linear equations. The roots of the determinant of these equations give estimates of the first $3M_p^3$ eigenvalue frequencies. The corresponding eigenvectors are $U_j^{(\alpha\beta\gamma)}$ from which the displacement field within the unit cell is reconstituted. The stress variation in the unit cell is obtained from Eq. $(6)^2$. The following example illustrates this procedure; as has been proved in Ref. 11, the resulting Fourier series expression converges at a rate that is faster than the corresponding Rayleigh quotient. The Appendix outlines the basic equations in matrix form, for elastic ellipsoidal inclusions periodically distributed within an elastic matrix, providing also the dispersion curves for elliptical fibers in an elastic matrix.

A. Example: A two-layered composite

To evaluate the effectiveness and accuracy of the mixed variational method, consider a layered composite (Fig. 1) with harmonic longitudinal stress waves traveling perpendicular to the layers. The displacement u and stress σ are approximated by

$$\bar{u} = \sum_{\alpha=-M}^{+M} U^{(\alpha)} e^{i(qx+2\pi\alpha x/a)}, \quad \bar{\sigma} = \sum_{\alpha=-M}^{+M} S^{(\alpha)} e^{i(qx+2\pi\alpha x/a)}. \tag{7}$$

In these equations, a is the periodicity length. Substituting these into Eq. $(6)^2$ we obtain S^α in terms of U^α. The resulting equations are then substituted into Eq. $(6)^1$, providing a set of M_p linear homogeneous equations, the roots of whose determinant give the first M_p eigenvalue frequencies for a given wave number q.

The exact dispersion relation for 1D longitudinal wave propagation in a periodic layered composite has been given by Rytov,[7]

$$\cos(qa) = \cos(\omega h_1/c_1)\cos(\omega h_2/c_2) - \Gamma \sin(\omega h_1/c_1)\sin(\omega h_2/c_2), \tag{8}$$

$$\Gamma = (1+\kappa^2)/(2\kappa), \quad \kappa = \rho_1 c_1/(\rho_2 c_2), \tag{9}$$

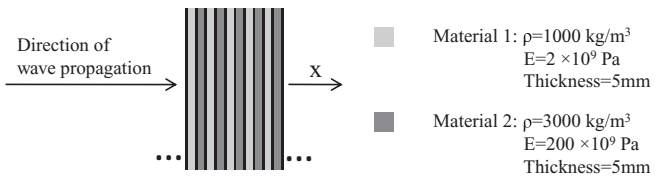

FIG. 1. Schematic of a layered composite.

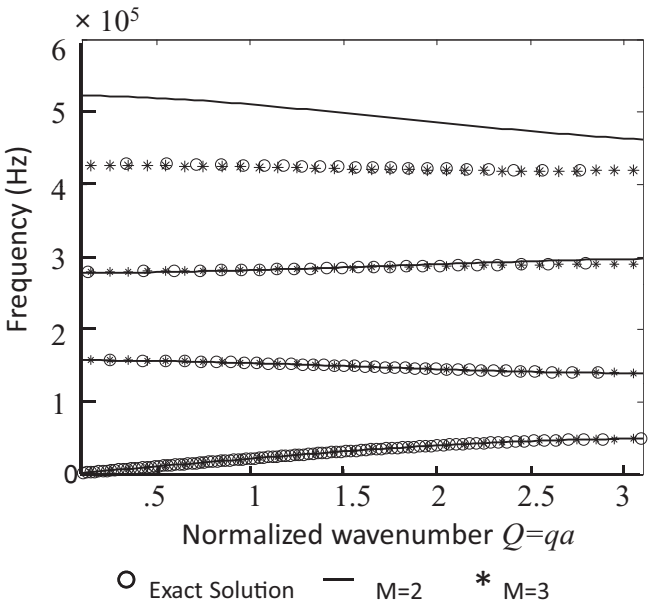

FIG. 2. Frequency–wave number dispersion relations; comparison of approximate and exact results for the first four branches.

where h_i is the thickness, ρ_i is the density, and c_i is the longitudinal wave velocity of the ith layer ($i = 1,2$) in a unit cell. In Fig. 2 we compare the frequency–wave number dispersion relations obtained by this mixed variational method and the exact solution.

The first four modes are compared in Fig. 2. It can be seen that the mixed method gives accurate results for the first three modes when $M_p = 5$ ($M = 2$) terms are used to approximate the displacement and stress. The fourth mode is inaccurate for the $M = 2$ calculation but as the number of terms in the expansion is increased to $M_p = 7$ ($M = 3$), the results converge to those obtained from the exact solution.

Since the exact dispersion relations are available for only fairly simple geometries like layered composites, the mixed variational formulation provides an attractive and effective method to calculate the eigenfrequencies and eigenvectors associated with three-dimensionally periodic composites. In the next section we present a four-layered example where the dispersion curves are calculated from the mixed variational formulation.

B. Example: A four-layered composite

We present a four-layered case where a heavy and stiff material is placed between thin layers of a soft and light material and the whole assembly is in a heavy and stiff matrix. The case is similar to Refs. 15–17 where the heavy and stiff central layer produces localized resonances which give rise to a low-frequency negative passband.

Figure 3(a) shows the schematic diagram of a unit cell of the four-layered composite considered. Figure 3(b) shows the dispersion curve for the composite. The first two propagating modes have been pushed to low frequencies and a significant stop band exists between the second and the third passbands. Figure 4 shows the real part of the displacement profile along the unit cell at $Q = 0.5$ on branch P_2. It can be seen that there

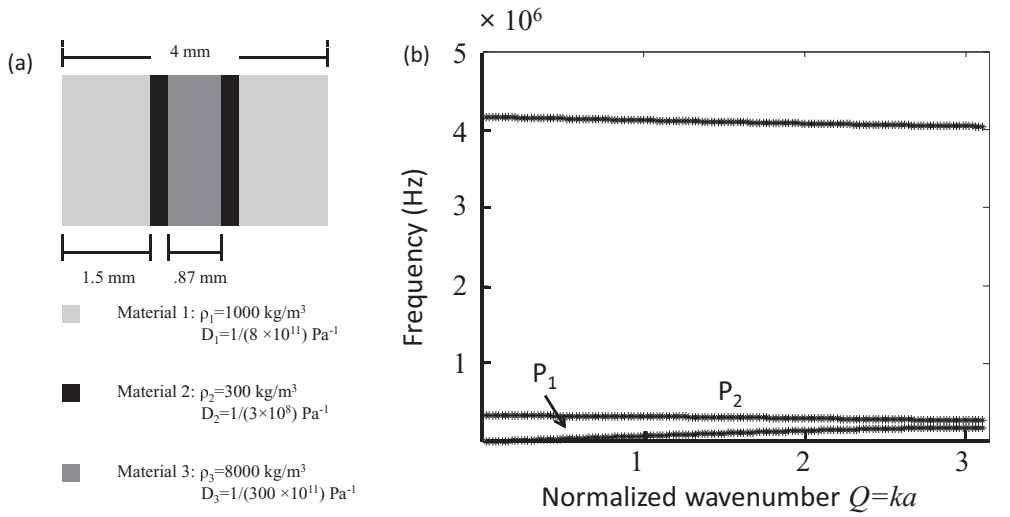

FIG. 3. Four-layered composite. (a) Schematic of a unit cell. (b) Frequency–wave number dispersion curve.

is a rigid-body motion of the central layer with respect to the matrix.

III. HOMOGENIZATION BY INTEGRATION OF FIELD VARIABLES

Many studies of Floquet-waves in composite materials seek to extract effective constitutive properties from computed solutions for waves propagating freely through the material. This section develops a prescription which is easily applied and delivers effective properties that are guaranteed by their construction to produce the exact dispersion relation as necessary condition without any approximation. It is presented in the one-dimensional context of the present work but it can be extended directly to two- and three-dimensional problems.

For harmonic waves traveling in a layered composite with a periodic unit cell $\Omega = \{x: -a/2 \leqslant x < a/2\}$, the field variables (displacement, velocity, strain, stress, and momentum) take the following Bloch form:

$$u(x,t) = U(x)e^{i(qx-\omega t)}, \quad v(x,t) = V(x)e^{i(qx-\omega t)}, \tag{10}$$

$$\epsilon(x,t) = E(x)e^{i(qx-\omega t)}, \quad \sigma(x,t) = \Sigma(x)e^{i(qx-\omega t)}, \tag{11}$$

$$p(x,t) = P(x)e^{i(qx-\omega t)}, \tag{12}$$

where functions $U(x)$, $\epsilon(x)$, $V(x)$, $E(x)$, $\Sigma(x)$, and $P(x)$ are periodic with the periodicity of the unit cell. The dynamic equilibrium and the strain-rate/velocity relations give

$$\nabla\sigma + i\omega p = 0, \quad \nabla v + i\omega\epsilon = 0, \tag{13}$$

where ∇ denotes differentiation with respect to x.

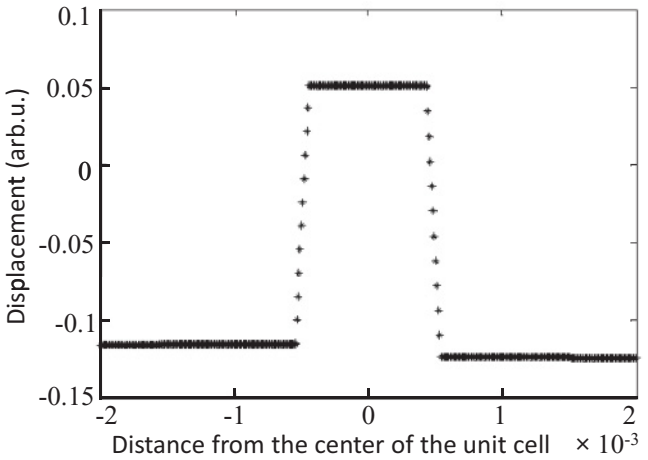

FIG. 4. Displacement profile along the unit cell at $Q = 0.5$, $f = 25.8$ kHz.

A. Effective properties

Multiply Eqs. (13) by e^{-iqX} and use Eqs. (10)–(12) to obtain

$$\nabla(\Sigma(x)e^{iq(x-X)}) + i\omega P(x)e^{iq(x-X)} = 0, \tag{14}$$

$$\nabla(V(x)e^{iq(x-X)}) + i\omega E(x)e^{iq(x-X)} = 0. \tag{15}$$

Introduce the change of variable $y = x - X$ to obtain

$$\nabla_y(\Sigma(X+y)e^{iqy}) + i\omega P(X+y)e^{iqy} = 0, \tag{16}$$

$$\nabla_y(V(X+y)e^{iqy}) + i\omega E(X+y)e^{iqy} = 0. \tag{17}$$

Average the above equation with respect to X over the unit cell to arrive at

$$\nabla_y(\bar{\Sigma}e^{iqy}) + i\omega\bar{P}e^{iqy} = 0, \tag{18}$$

$$\nabla_y(\bar{V}e^{iqy}) + i\omega\bar{E}e^{iqy} = 0, \tag{19}$$

where any one of the barred quantities is defined as

$$\bar{G} = \frac{1}{a}\int_{-a/2}^{+a/2} G(X)dX. \tag{20}$$

Note that the overall field variables defined according to (20) satisfy the overall field equations, as is ensured by Eqs. (18) and (19), from which we have

$$\bar{\Sigma} + \frac{\omega}{q}\bar{P} = 0, \quad \bar{V} + \frac{\omega}{q}\bar{E} = 0. \tag{21}$$

Now define the *mean* constitutive relations as

$$\bar{\Sigma} = C^{\text{eff}}\bar{E}, \quad \bar{P} = \rho^{\text{eff}}\bar{V}. \tag{22}$$

Then, for the four linear and homogeneous equations (21) and (22) to admit nontrivial solutions for the overall effective field quantities, $\bar{\Sigma}$, $\bar{P}$, $\bar{V}$, and $\bar{E}$, we must have

$$\frac{C^{\text{eff}}}{\rho^{\text{eff}}} = \left(\frac{\omega}{q}\right)^2, \tag{23}$$

which gives the dispersion relations. We emphasize that this homogenization procedure delivers the exact dispersion relation (23) as a necessary condition without any need for further adjustment. We also mention that the effective parameters defined by (22) are real-valued only if the unit cell is symmetric. For nonsymmetric unit cells, the coupling among the field variables renders the effective stiffness C^{eff} and mass density ρ^{eff}, defined by (22), complex valued.

IV. HOMOGENIZATION OF LAYERED COMPOSITES

To illustrate the above method of homogenization, the numerical example of Fig. 1 is considered again. Since the exact solution in the form of dispersion relation and displacement and stress fields exists for this simple layered case, it will be shown by way of comparison that results of the homogenization based on the approximate mixed variational formulation rapidly converge to those based on the exact solution, suggesting that the approximate method may be confidently used to estimate the effective properties of two- and three-dimensionally periodic composites for which exact solutions cannot be constructed.

Figure 2 shows the dispersion curves corresponding to the first four propagating branches, for the layered composite shown in Fig. 1. These are calculated using the exact solution and the mixed variational formulation. For the frequency band corresponding to each of these branches, Eq. (8) yields real (normalized) wave numbers ($0 \leqslant Q = qa \leqslant \pi$) and a wave

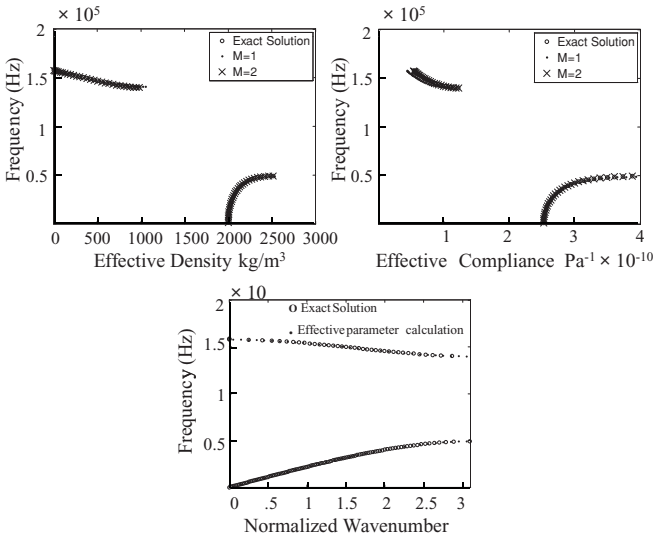

FIG. 5. Effective parameters for layered composite: effective density (ρ^{eff}), effective compliance (D^{eff}), and the dispersion curve calculated from effective parameters (bottom panel).

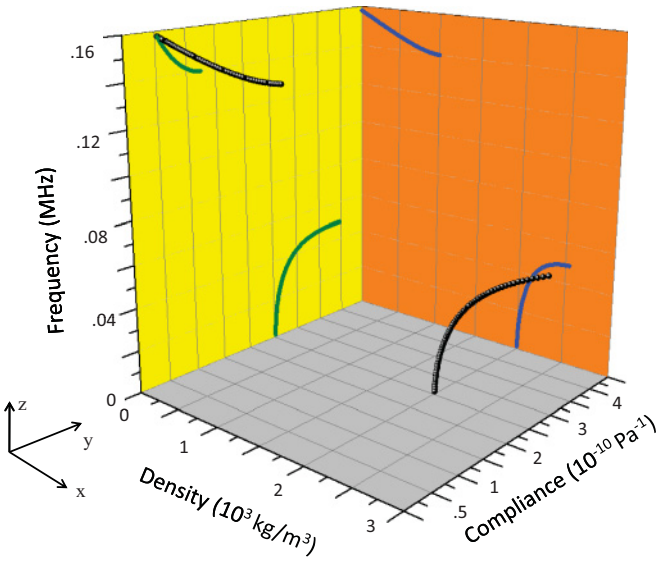

FIG. 6. (Color) Dynamic Ashby chart representation of frequency-dependent effective compliance and density corresponding to the three microstructures shown in Fig. 1, where volume fraction and properties of the constituents within the unit cell are kept constant.

at a corresponding frequency travels undamped through the composite. Frequency bands within which no propagating mode exists constitute the stop bands. The normalized wave numbers satisfying Eq. (8) for these frequencies take on the form $Q = (2n+1)\pi \pm i\alpha$ or $Q = 2n\pi \pm i\alpha$, where α is a positive real number and n is an integer. These modes are nonpropagating and their energy is trapped within the first few layers due to multiple reflections. As a result, the amplitude of a nonpropagating wave decreases exponentially with propagation distance. Although an infinite number of propagating branches exist as the frequency under consideration is increased, meaningful homogenization can be carried out only for low-frequency branches, below the diffraction limit. Therefore, only the first two propagating branches are considered in what follows.

Figure 5 shows the effective parameters for the case of the two-layered composite. It can be seen that the homogenization results from the approximate method are in very good agreement with those from the exact solution. The top left panel of Fig. 5 shows the variation of the effective density, and the top right that of the effective compliance ($D^{\text{eff}} = 1/C^{\text{eff}}$) of the composite, as functions of frequency. It can be seen that the effective density and compliance are nearly constant for

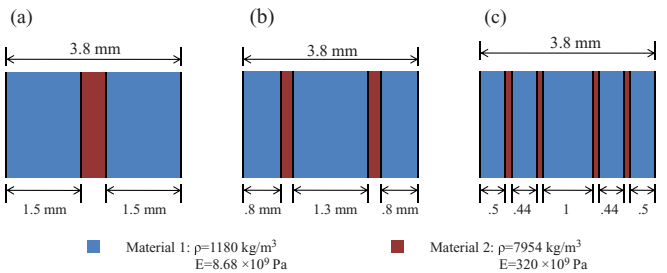

FIG. 7. (Color online) Schematic of the architectures used for comparison.

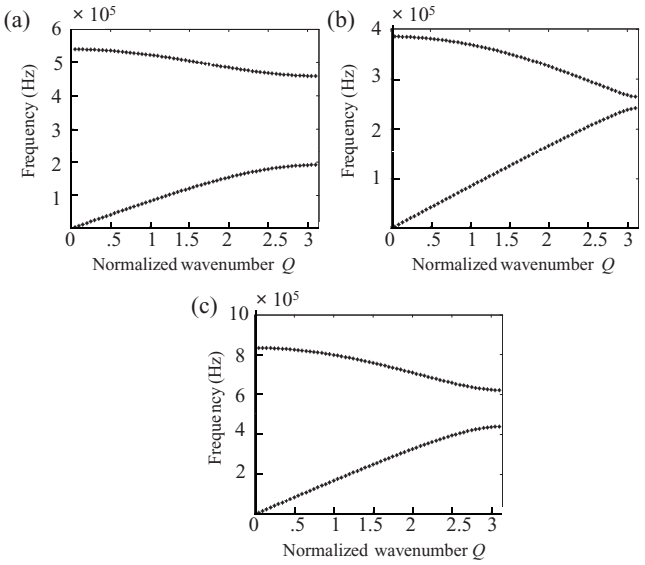

FIG. 8. Dispersion curves for considered microarchitectures.

low frequencies and are equal to the volume average of those of the individual constituents of the unit cell. This is expected since at low frequencies the Bloch wavelength is much larger than the thickness of individual layers and the response of the composite is nearly static. The bottom panel of Fig. 5 shows the dispersion curves, based on the calculated effective parameters $[Q = a(\omega^2 \rho^{\text{eff}} D^{\text{eff}})^{1/2}]$. It can be seen from the panel that the calculated effective parameters exactly satisfy the dispersion relation of Fig. 2.

A. Dynamic Ashby chart representation

The effective material properties calculated above define propagation, reflection, and refraction of stress waves in the composite. They may be nicely dislayed in a three-dimensional chart, as shown in Fig. 6. We refer to charts of this kind as dynamic Ashby charts. In general, dynamic Ashby charts are

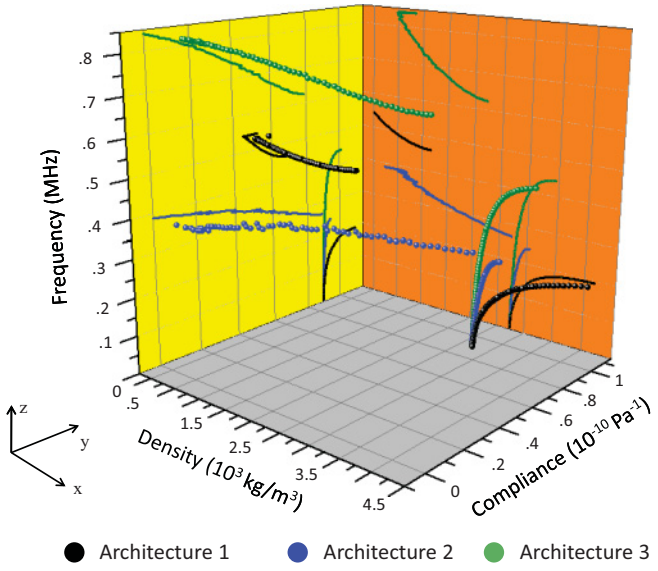

FIG. 9. (Color) Dynamic Ashby chart: effect of microarchitecture on dynamic properties.

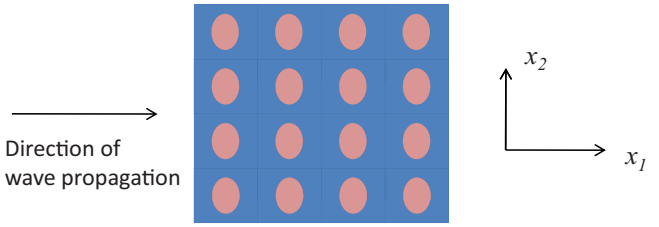

FIG. 10. (Color online) Schematic of the 2D plane stress case of elliptic inclusions uniformly distributed in an elastic matrix.

obtained from the corresponding static ones (associated with zero frequency), augmented with additional axes (representing frequency and wave vector) to account for the microstructural dependence of the overall dynamic properties of the material.

In Fig. 6, the 3D trajectory (black spheres) shows the effective density and compliance as functions of frequency. Its projection on the $y-$z plane (green curve) and $x-$z plane (blue curve) respectively shows the variation of the effective compliance and density with the wave frequency.

B. Microarchitectural control of dynamic properties

In a standard Ashby chart the composite is represented by a single point that corresponds to its considered quasistatic properties. The effective dynamic properties of the composite, however, can take on a broad range of values depending on its microarchitecture, that is, depending on the manner by which the composite's constituents are distributed within its unit cell. This is illustrated by comparing the dynamic trajectories of three simple architectures shown in Fig. 7 with the same static overall mass density and compliance; i.e., all three trajectories start from the same point in the corresponding static Ashby chart.

Starting with the same linear fraction of each of the two materials, measured per unit length, we consider the dynamic effects of their distribution within a unit cell according to three different architectures, denoted as (1), (2), and (3) in Fig. 7.

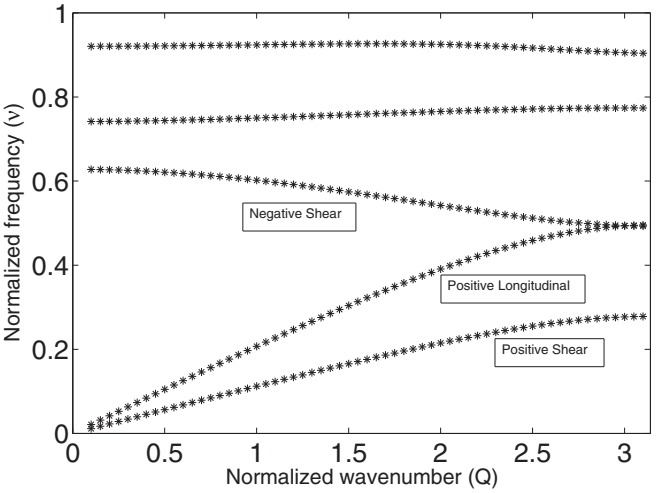

FIG. 11. Dispersion curves for a composite consisting of elliptical fibers periodically distributed in an elastic matrix. The lower first two curves are for the shear and longitudinal waves with the corresponding phase and group velocities parallel. The third curve is a negative shear-wave branch with antiparallel phase and group velocities.

Figure 8 shows the dispersion curves for the first two propagating branches for the three cases. As material is redistributed from case (1) to case (2), the low-frequency stop band is decreased. For architecture (3) with a finer distribution of the two constituent materials, the overall dynamic response corresponds to higher frequencies as compared to those of the first two architectures.

Figure 9 shows the corresponding trajectories for the three architectures in the dynamic Ashby chart. All three trajectories start at the same point on the zero-frequency plane, with effective density $= 2742$ kg/m^3 and effective compliance $= 8.94 \times 10^{-11}$ Pa^{-1}, calculated according to the volume fraction of the constituents. It can be seen that the trajectories of effective density and compliance for the three architectures pass through significantly different regions within this three-dimensional dynamic Ashby chart. By changing the distribution scale of the individual constituent materials, it is seen that architecture (3) exhibits a relatively static response at frequencies up to about 300 kHz, but its dynamic response is frequency dependent at higher frequencies. This illustrates how one can change the architecture at nano-, micro-, meso-, and macro-scales to manage stress waves over many windows of frequencies.

V. CONCLUSIONS

For Floquet waves in a periodic elastic composite, a homogenization method is presented. It is adapted from a more general approach[6] and is based on the integration of field variables over a unit cell. The resulting effective parameters satisfy the overall field equations, yield the exact dispersion relation as a necessary condition, and are spatially nondispersive in the long-wavelength limit. The technique is used to calculate the effective properties of a two-layered composite, employing both the exact solution and an approximate solution[8] using a mixed variational formulation. It is shown that the effective parameters calculated from the approximate method quickly converge to the homogenization results based on the exact solution. The results are presented in the context of general augmented Ashby-type charts, referred to as dynamic Ashby charts, that provide an effective tool for the representation of frequency-dependent dynamic effective properties of composites.

ACKNOWLEDGMENTS

This research has been conducted at the Center of Excellence for Advanced Materials (CEAM) at the University of California, San Diego. This work has been supported by DARPA AFOSR Grant No. FA9550-09-1-0709 to the University of California, San Diego.

APPENDIX A: EXPLICIT EQUATIONS FOR THE CALCULATION OF THE DISPERSION RELATION FOR A 3D CASE: ELLIPSIODAL INCLUSIONS IN ELASTIC MATRIX

For illustration of the explicit equations for a 3D case, consider a composite whose unit cell is a rectangular parallelepiped with dimensions a_i in directions x_i $(i = 1,2,3)$, respectively. Let the cell consist of two material constituents, the matrix and an ellipsoidal inclusion. The inclusion is centered with respect to the unit cell in such a manner that its three principal axes are each placed parallel to the corresponding sides of the unit cell so that it has diameters b_i in directions x_i $(i = 1,2,3)$, respectively.

For this case, Eqs. (6) can be written in the following matrix form:

$$\left[\mathbf{H}\mathbf{\Phi}^{-1}\mathbf{H}^{*} - \frac{\nu^2}{d}\mathbf{\Omega}\right]\mathbf{U} = 0, \tag{A1}$$

where matrices $\mathbf{H}$, $\mathbf{\Phi}$, and $\mathbf{\Omega}$ are defined as follows:

$$[\mathbf{H}] = \begin{bmatrix} \mathcal{H}_1 & \mathcal{H}_2 & \mathcal{H}_3 & 0 & 0 & 0 \\ 0 & \mathcal{H}_1 & 0 & \mathcal{H}_2 & \mathcal{H}_3 & 0 \\ 0 & 0 & \mathcal{H}_1 & 0 & \mathcal{H}_2 & \mathcal{H}_3 \end{bmatrix},$$

where $\mathcal{H}_1$, $\mathcal{H}_2$, and $\mathcal{H}_3$ are $(2M+1)^3 \times (2M+1)^3$ matrices defined in the following manner: For $\alpha = \delta$, $\beta = \mu$, and $\gamma = \tau$, and with $Q_j = q_j a_j$ (no sum),

$$\begin{aligned} \mathcal{H}_1(I_1,J_1) &= -i(Q_1 + 2\pi\alpha), \\ \mathcal{H}_2(I_1,J_1) &= -i(Q_2 + 2\pi\beta)n_0, \\ \mathcal{H}_3(I1,J_1) &= -i(Q_3 + 2\pi\gamma)m_0. \end{aligned} \tag{A2}$$

For $\alpha \neq \delta$, $\beta \neq \mu$, $\gamma \neq \tau$,

$$\mathcal{H}_1(I_1,J_1) = \mathcal{H}_2(I_1,J_1) = \mathcal{H}_3(I_1,J_1), \tag{A3}$$

where $I_1 = (\alpha + 1 + M) + (\beta + M)(2M+1) + (\gamma + M)(2M+1)^2$ and $J_1 = (\delta + 1 + M) + (\mu + M)(2M+1) + (\tau + M)(2M+1)^2$; $\delta,\mu,\tau = 0, \pm 1, \pm 2, \ldots, \pm M$.

$$[\mathbf{\Omega}] = \begin{bmatrix} \bar{\mathbf{\Omega}} & 0 & 0 \\ 0 & \bar{\mathbf{\Omega}} & 0 \\ 0 & 0 & \bar{\mathbf{\Omega}} \end{bmatrix}$$

and

$$[\mathbf{\Phi}] = \begin{bmatrix} \bar{\mathbf{\Phi}}_{1111} & 0 & 0 & \bar{\mathbf{\Phi}}_{1122} & 0 & \bar{\mathbf{\Phi}}_{1133} \\ 0 & 4\bar{\mathbf{\Phi}}_{1212} & 0 & 0 & 0 & 0 \\ 0 & 0 & 4\bar{\mathbf{\Phi}}_{1313} & 0 & 0 & 0 \\ \bar{\mathbf{\Phi}}_{1122} & 0 & 0 & \bar{\mathbf{\Phi}}_{2222} & 0 & \bar{\mathbf{\Phi}}_{2233} \\ 0 & 0 & 0 & 0 & 4\bar{\mathbf{\Phi}}_{2323} & 0 \\ \bar{\mathbf{\Phi}}_{1133} & 0 & 0 & \bar{\mathbf{\Phi}}_{2233} & 0 & \bar{\mathbf{\Phi}}_{3333} \end{bmatrix},$$

where $\bar{\mathbf{\Omega}}$ and $\bar{\mathbf{\Phi}}_{ijkl}$ are $(2M+1)^3 \times (2M+1)^3$ matrices defined in the following manner:

$$\begin{aligned} \bar{\mathbf{\Omega}}(I_1,J_1) &= 1 \text{ if } \alpha = \delta, \ \beta = \mu, \text{ and } \gamma = \tau; \\ &= \left[\frac{\pi}{2}\right]^{3/2} \frac{\theta - 1}{\bar{n}_1 + \bar{n}_2\theta} \frac{n_2 m_2 l_2 J_{3/2}(R)}{R^{3/2}} \quad \text{otherwise;} \end{aligned} \tag{A4}$$

where $J_{3/2}$ is a Bessel function of the first kind of order 3/2 and its argument R is given by

$$R = \pi\left[n_2^2(\delta - \alpha)^2 + m_2^2(\mu - \beta)^2 + l_2^2(\tau - \gamma)^2\right]^{1/2}. \tag{A5}$$

For $I_1 \neq J_1$, $\bar{\mathbf{\Phi}}_{ijkl}$ is obtained if one substitutes $(\gamma_{ijkl} - 1)R_{ijkl}/(\bar{n}_1 + \bar{n}_2\gamma_{1111})$ for $\frac{\theta - 1}{\bar{n}_1 + \bar{n}_2\theta}$ in the expression for $\bar{\mathbf{\Omega}}(I_1,J_1)$, and for $I_1 = J_1$ one has

$$\bar{\mathbf{\Phi}}_{ijkl} = \frac{(\bar{n}_1 + \bar{n}_2\gamma_{ijkl})R_{ijkl}}{(\bar{n}_1 + \bar{n}_2\gamma_{1111})}. \tag{A6}$$

The following notation is used in the above expressions:

$$\nu^2 = \frac{\omega^2 a_1^2 \bar{\rho}}{\bar{C}_{1111}}, \quad \bar{\rho} = \rho^{(1)}\bar{n}_1 + \rho^{(2)}\bar{n}_2, \quad \bar{C}_{1111} = C^{(1)}_{1111}\bar{n}_1 + C^{(2)}_{1111}\bar{n}_2,$$
$$\bar{n}_1 = 1 - \bar{n}_2, \quad \bar{n}_2 = \frac{\pi b_1 b_2 b_3}{6 a_1 a_2 a_3}, \quad \theta = \frac{\rho^{(2)}}{\rho^{(1)}}, \quad n_2 = \frac{b_1}{a_1}, \quad m_2 = \frac{b_2}{a_2},$$
$$l_2 = \frac{b_3}{a_3}, \quad n_0 = \frac{a_1}{a_2}, \quad m_0 = \frac{a_1}{a_3}, \quad \gamma_{jklm} = \frac{D^{(2)}_{jklm}}{D^{(1)}_{jklm}},$$
$$R_{jklm} = \frac{D^{(1)}_{jklm}}{D^{(1)}_{1111}}, \quad d = 1/(\bar{C}_{1111}\bar{D}_{1111}), \quad \bar{D}_{1111} = D^{(1)}_{1111}\bar{n}_1 + D^{(2)}_{1111}\bar{n}_2, \tag{A7}$$

where $j,k,l,m = 1,2,3$; a_1, a_2, a_3 are the dimensions of the unit cell; and b_1, b_2, b_3 are the diameters of the ellipsoidal inclusion in the coordinate directions x_1, x_2, and x_3, respectively. Superscript (1) refers to the matrix and (2) refers to the inclusion. The tensors γ_{jklm} and R_{jklm} are the compliances of the inclusion and matrix materials normalized with respect to $D^{(1)}_{1111}$. For the case of isotropic inclusions and isotropic matrix materials, tensors $C^{(1)}_{ijkl}, C^{(2)}_{ijkl}$ and their inverses $D^{(1)}_{ijkl}, D^{(2)}_{ijkl}$ are determined by four independent elastic constants (two for the matrix and two for the inclusion). In terms of the Young modulus and Poisson's ratio, E and ν, the elasticity tensor of an isotropic material is given by

$$C_{ijkl} = \frac{E}{2(1+\nu)}\left[\frac{2\nu}{(1-2\nu)}\delta_{ij}\delta_{kl} + (\delta_{ik}\delta_{jl} + \delta_{il}\delta_{jk})\right]. \tag{A8}$$

The corresponding shear modulus then is $\mu = E/2(1+\nu)$.

The above treatment explicitly outlines the basic equations involved in the mixed variational formulation for the most general 3D case of ellipsoidal inclusions periodically distributed within an elastic matrix. No restriction is imposed on the elasticity of the matrix or inclusions. The plane stress case is obtained at the limit when the dimension of the unit cell (and the ellipsoid diameter) in the thickness direction (x_3) is negligibly small compared to the other two direction (Fig. 10). In this case displacements in only the x_1 and x_2 directions are considered and the only nonzero stresses are those which are in the plane x_1-x_2.

For this case, we have calculated the first five branches of the dispersion curves for isotropic fibers within an isotropic elastic matrix (Fig. 11). The relevant dimensional relations are $a_1 = a_2, b_1 = 0.5a_1, b_2 = 0.75a_2$. The wave vector is in the x_1 direction. The Young's modulus of the inclusion is 100 times the modulus of the matrix ($E^{(2)} = 100E^{(1)}$), and its density is 3 times the density of the matrix ($\rho^{(2)} = 3\rho^{(1)}$). Poisson's ratio for the matrix and the inclusion are 0.4 and 0.3, respectively. The results shown in Fig. 11 are for an approximation of $M = 2$. The lower first two curves in this figure are for the shear (lowest; particle displacement normal to the wave vector in the x_2 direction) and longitudinal (particle displacement parallel to the wave vector, in the x_1 direction) waves with the corresponding phase and group velocities parallel to one another (positive branches), whereas the third curve is a negative shear-wave branch with antiparallel phase and group velocities.

*Corresponding author: ansrivas@ucsd.edu

[1] J. B. Pendry, J. Mod. Opt. **41**, 209 (1994).
[2] J. B. Pendry, J. Phys. Condens. Matter **8**, 1085 (1996).
[3] D. R. Smith and J. B. Pendry, J. Opt. Soc. Am. B **23**, 391 (2006).
[4] A. V. Amirkhizi and S. Nemat-Nasser, Smart Materials and Structures **17**, 015042 (2008).
[5] A. V. Amirkhizi and S. Nemat-Nasser, C. R. Mecanique **336**, 24 (2008).
[6] J. R. Willis, Mech. Mater. **41**, 385 (2009).
[7] S. M. Rytov, Sov. Phys. Acoust. **2**, 68 (1956).
[8] S. Nemat-Nasser, J. Elasticity **2**, 73 (1972).
[9] S. Nemat-Nasser, F. C. L. Fu, and S. Minagawa, Int. J. Solids Struct. **11**, 617 (1975).
[10] S. Minagawa and S. Nemat-Nasser, Int. J. Solids Struct. **12**, 769 (1976).
[11] I. Babuška and J. E. Osborn, Math. Comput. **32**, 991 (1978).
[12] M. F. Ashby, *Materials Selection in Mechanical Design* (Butterworth-Heinemann, Oxford, 2005).
[13] V. G. Veselago, Phys. Usp. **10**, 509 (1968).
[14] D. R. Smith, W. J. Padilla, D. C. Vier, S. C. Nemat-Nasser, and S. Schultz, Phys. Rev. Lett. **84**, 4184 (2000).
[15] P. Sheng, X. X. Zhang, Z. Liu, and C. T. Chan, Physica B **338**, 201 (2003).
[16] Z. Liu, C. T. Chan, and P. Sheng, Phys. Rev. B **71**, 014103 (2005).
[17] G. W. Milton and J. R. Willis, Proc. R. Soc. London A **463**, 855 (2007).
[18] S. Gonella and M. Ruzzene, Int. J. Solids Struct. **45**, 2897 (2008).
[19] M. Hussein, M. Ruzzene, M. Leary, J. Durrie, and B. Davis, Proc. ASME **IMECE2008-68246**, 1 (2008).